Sandia National Laboratories

SAND2015-7334C

Optimization-Based Mesh Correction

M. D'Elia, D. Ridzal, K. Peterson, P. Bochev

Sandia National Laboratories

M. Shashkov

Los Alamos National Laboratory

MultiMat

September 9, 2015

U.S. DEPARTMENT OF ENERGY

Sandia National Laboratories is a multi-program laboratory managed and operated by Sandia Corporation, a wholly owned subsidiary of Lockheed Martin Corporation, for the U.S. Department of Energy's National Nuclear Security Administration under contract DE-AC04-94AL85000.

Motivation

Divergence Free Lagrangian Motion

- Given cell κ at initial time t^0

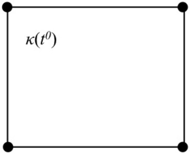

Motivation

Divergence Free Lagrangian Motion

- Given cell κ at initial time t^0
- Compute nodal displacement from velocity field $\mathbf{u}$

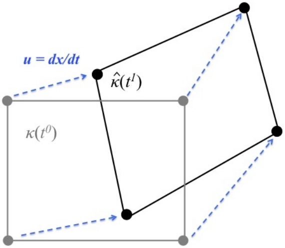

Motivation

Divergence Free Lagrangian Motion

- Given cell κ at initial time t^0
- Compute nodal displacement from velocity field $\mathbf{u}$
- Updated cell $\hat{\kappa}(t^1)$ has both temporal and spatial errors

Violation of volume preservation

$$\frac{d}{dt}\int_{\kappa(t)} dV \neq 0$$

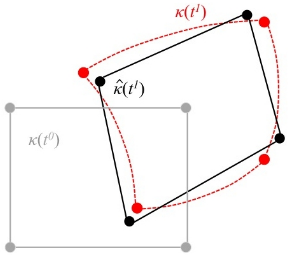

Motivation

Divergence Free Lagrangian Motion

- Given cell κ at initial time t^0
- Compute nodal displacement from velocity field $\mathbf{u}$
- Updated cell $\hat{\kappa}(t^1)$ has both temporal and spatial errors

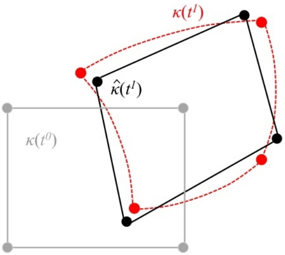

Violation of volume preservation

$$\frac{d}{dt}\int_{\kappa(t)} dV \neq 0$$

Consider $\rho = const$

Let cell mass $M_\kappa(t) = \int_{\kappa(t)} \rho dV$ and cell density $\rho_\kappa = \frac{M_\kappa(t)}{|\kappa(t)|}$,
where $|\kappa(t)| = \int_{\kappa(t)} dV$

$$\rho_\kappa(t^1) = \frac{M_\kappa(t^1)}{|\hat{\kappa}(t^1)|} \neq \frac{M_\kappa(t^0)}{|\kappa(t^0)|} = \rho_\kappa(t^0)$$

Cannot maintain a constant density!

Geometric Conservation Law (GCL)

$$\frac{d}{dt}\int_{\kappa_i(t)} dV = \int_{\partial\kappa_i(t)} \mathbf{u}\cdot\mathbf{n}\,ds$$

Some recent work:

Use more Lagrangian points

- Enforces GCL approximately

Lauritzen, Nair, Ullrich, A conservative semi-Lagrangian multi-tracer transport scheme on the cubed-sphere grid, *JCP* 229/5 (2010).

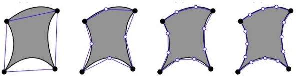

Heuristic mesh adjustment procedure

- No theoretical assurance of completion

Arbogast, Huang, A fully mass and volume conserving implementation of a characteristic method for transport problems, *SISC* 28 (6) (2006).

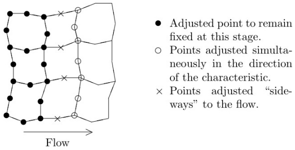

Monge-Ampere trajectory correction

- Requires nontrivial solution of the nonlinear MAE

Cossette, Smolarkiewicz, Charbonneau, The Monge-Ampere trajectory correction for semi-Lagrangian schemes, JCP (2014).

$$\tilde{\mathbf{p}}_{ij}^{corr} = \tilde{\mathbf{p}}_{ij} + (t - t_n)\nabla\phi;$$

$$\det\frac{\partial\mathbf{p}_{ij}}{\partial x} = 1$$

Optimization-Based Solution

Given a *source mesh* $\widetilde{K}(\Omega)$, and *desired cell volumes* $\boldsymbol{c}_0 \in \mathbb{R}^m$ such that

$$\sum_{i=1}^{m} c_{0,i} = |\Omega| \quad \text{and} \quad c_{o,i} > 0 \forall i = 1, ..., m$$

Find a *volume compliant mesh* $K(\Omega)$ such that

1. $K(\Omega)$ has the same connectivity as the source mesh
2. The volumes of its cells match the volumes prescribed in $\boldsymbol{c}_0$
3. Every cell $\kappa_i \in K(\Omega)$ is valid or convex
4. Boundary points in $K(\Omega)$ correspond to boundary points in $\widetilde{K}(\Omega)$

For Quadrilateral Cells We Need

Oriented volume of quad cell:

$$\boldsymbol{c}_i(K(\Omega)) = \frac{1}{2}\left((x_{i,1}-x_{i,3})(y_{i,2}-y_{i,4})+(x_{i,2}-x_{i,4})(y_{i,3}-y_{i,1})\right)$$

Partitioning of quad into triangles:

$$(a_r, b_r, c_r) = \begin{cases} (1,2,4) & r=1 \\ (2,3,4) & r=2 \\ (1,3,4) & r=3 \\ (1,2,3) & r=4. \end{cases}$$

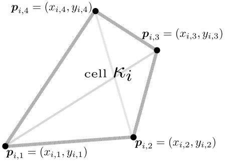

Oriented volume of triangle cell:

$$\boldsymbol{t}_i^r(K(\Omega)) = \frac{1}{2}(x_{i,a_r}(y_{i,c_r}-y_{i,b_r})-x_{i,b_r}(y_{i,a_r}-y_{i,c_r})-x_{i,c_r}(y_{i,b_r}-y_{i,a_r})).$$

Convexity indicator for a quad cell:

$$\mathcal{I}_i(K(\Omega)) = \begin{cases} 1 & \text{if } \forall \boldsymbol{t}_i^r \in \kappa_i, |\boldsymbol{t}_i^r| > 0 \\ 0 & \text{otherwise} \end{cases}$$

Optimization Problem

Objective:

Mesh distance $J_0(\boldsymbol{p}) = \frac{1}{2} d\big(K(\Omega), \tilde{K}(\Omega)\big)^2 = |\boldsymbol{p} - \tilde{\boldsymbol{p}}|_{l^2}^2$

Constraints:

(1) Volume equality $\forall \kappa_i \in K(\Omega), |\kappa_i| = c_{0,i}$

(2) Cell convexity $\forall \kappa_i \in K(\Omega), \forall t_i^r \in \kappa_i, |t_i^r| > 0$

(3) Boundary compliance $\forall p_i \in \partial\Omega, \gamma(p_i) = 0$

Nonlinear programming problem (NLP)

$\boldsymbol{p}* = \text{arg min}\big\{J_0(\boldsymbol{p}) \text{ subject to (1),(2), and (3)}\big\}$

Simplified Formulation

For polygonal domains

- boundary compliance can be subsumed in the volume constraint
- convexity can be enforced weakly by logarithmic barrier functions

Objective:

Mesh distance - log barrier
$$J(\boldsymbol{p}) = J_0(\boldsymbol{p}) - \beta \sum_{i=1}^{m} \sum_{r=1}^{4} \log \boldsymbol{t}_i^r(\boldsymbol{p})$$
$$J_0(\boldsymbol{p}) = |\boldsymbol{p} - \tilde{\boldsymbol{p}}|_{l^2}^2$$

Constraints:

(1) Volume equality $\forall \kappa_i \in K(\Omega), |\kappa_i| = c_{0,i}$

Simplified NLP

$$\boldsymbol{p}^* = \text{arg min}\{J(\boldsymbol{p}) \text{ subject to (1)}\}$$

Scalable Optimization Algorithm

Based on the inexact trust region sequential programming (SQP) method with key properties:

- Fast local convergence
- Use of 'inexact' solvers
- Requires efficient preconditioner

Linear systems of optimization iterate $\boldsymbol{p}^k$ are of the form

$$\begin{pmatrix} I & \nabla \boldsymbol{C}(\boldsymbol{p}^k)^T \\ \nabla \boldsymbol{C}(\boldsymbol{p}^k) & 0 \end{pmatrix} \begin{pmatrix} \boldsymbol{v}^1 \\ \boldsymbol{v}^2 \end{pmatrix} = \begin{pmatrix} \boldsymbol{b}^1 \\ \boldsymbol{b}^2 \end{pmatrix},$$

where $\boldsymbol{C}(\boldsymbol{p}^k)$ is a polynomial matrix function of coordinates.

Preconditioner

$$\pi^k = \begin{pmatrix} I & 0 \\ 0 & (\nabla \boldsymbol{C}(\boldsymbol{p}^k) \nabla \boldsymbol{C}(\boldsymbol{p}^k)^T + \varepsilon I)^{-1} \end{pmatrix}$$

- $\epsilon > 0$ small parameter $10^{-8}h$
- $\nabla \boldsymbol{C}(\boldsymbol{p}^k) \nabla \boldsymbol{C}(\boldsymbol{p}^k)^T$ formed explicitly
- Smoothed aggregation AMG used for inverse

Heinkenschloss, Ridzal, A matrix-free trust-region SQP method for equality constrained optimization SIOPT 24/3 (2000).

Scalablility Test

To challenge the algorithm we test performance as follows:

- Start with uniform $n \times n$ mesh and advance to final time using velocity field
- Apply algorithm to the deformed mesh at the final time using initial mesh volumes

Analytic Hessian

n	SQP	CG	GMRES tot.	GMRES av.	CPU	% ML time
64	5	15	101	2.8	2.475	66
128	4	9	106	4.1	8.799	78
256	5	5	130	5.0	45.733	83
512	6	1	100	3.8	184.446	83

Gauss-Newton Hessian

n	SQP	CG	GMRES tot.	GMRES av.	CPU	% ML time
64	5	5	64	2.5	1.666	63
128	4	4	79	3.8	6.466	82
256	5	5	126	4.8	43.241	86
512	6	6	100	3.8	183.697	86

- Almost constant GMRES iterations
- CPU per SQP iteration scales linearly with problem
- CPU and inner CG iteration counts are mesh independent
- The algorithm inherits its scalability from the AMG solver

Lagrangian Motion

Swirling velocity field:

$$\mathbf{u}(\mathbf{x}, t) = \begin{pmatrix} \cos\left(\frac{t\pi}{T}\right) \sin(\pi x)^2 \sin(2\pi y) \\ -\cos\left(\frac{t\pi}{T}\right) \sin(\pi y)^2 \sin(2\pi x) \end{pmatrix}$$

Use 8x8 mesh, $T = 8$, forward Euler for trajectories.

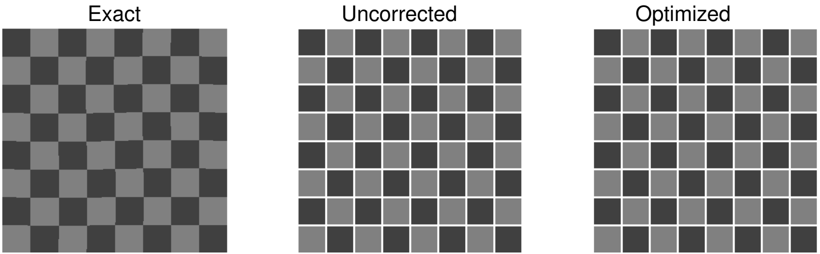

Lagrangian Motion

Swirling velocity field:

$$\mathbf{u}(\mathbf{x}, t) = \begin{pmatrix} \cos\left(\frac{t\pi}{T}\right) \sin(\pi x)^2 \sin(2\pi y) \\ -\cos\left(\frac{t\pi}{T}\right) \sin(\pi y)^2 \sin(2\pi x) \end{pmatrix}$$

Use 8x8 mesh, $T = 8$, forward Euler for trajectories.

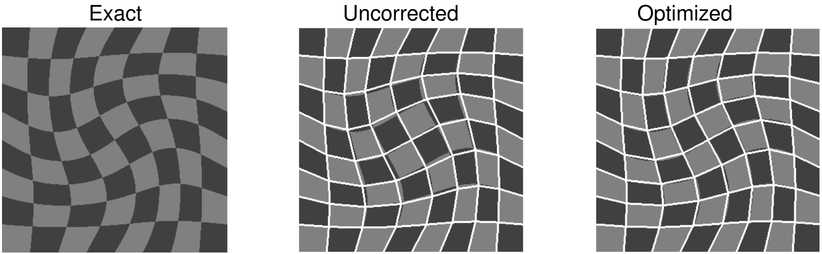

Lagrangian Motion

Swirling velocity field:

$$\mathbf{u}(\mathbf{x}, t) = \begin{pmatrix} \cos\left(\frac{t\pi}{T}\right) \sin(\pi x)^2 \sin(2\pi y) \\ -\cos\left(\frac{t\pi}{T}\right) \sin(\pi y)^2 \sin(2\pi x) \end{pmatrix}$$

Use 8x8 mesh, $T = 8$, forward Euler for trajectories.

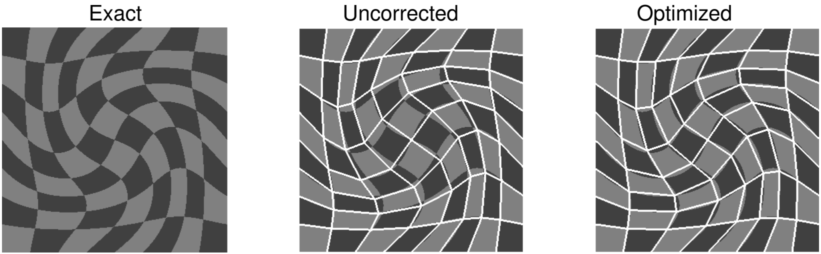

Lagrangian Motion

Swirling velocity field:

$$\mathbf{u}(\mathbf{x}, t) = \begin{pmatrix} \cos\left(\frac{t\pi}{T}\right) \sin(\pi x)^2 \sin(2\pi y) \\ -\cos\left(\frac{t\pi}{T}\right) \sin(\pi y)^2 \sin(2\pi x) \end{pmatrix}$$

Use 8x8 mesh, $T = 8$, forward Euler for trajectories.

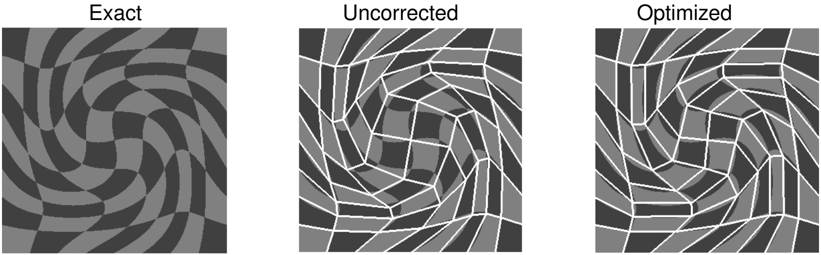

Lagrangian Motion

Swirling velocity field:

$$\mathbf{u}(\mathbf{x}, t) = \begin{pmatrix} \cos\left(\frac{t\pi}{T}\right)\sin(\pi x)^2 \sin(2\pi y) \\ -\cos\left(\frac{t\pi}{T}\right)\sin(\pi y)^2 \sin(2\pi x) \end{pmatrix}$$

Use 8x8 mesh, $T = 8$, forward Euler for trajectories.

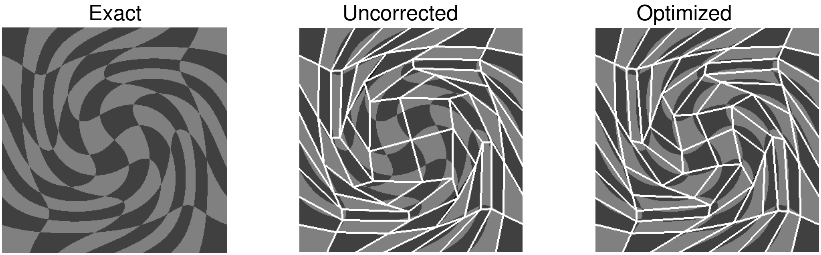

Improvements in Mesh Geometry

We observe significant improvements in the geometry of the corrected mesh:

- The shapes of the corrected cells are close to the exact Lagrangian shapes

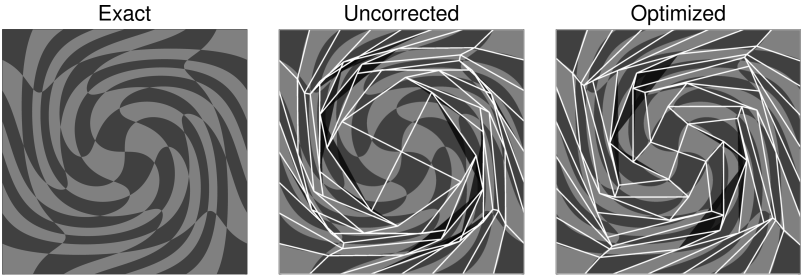

Improvements in Mesh Geometry

We observe significant improvements in the geometry of the corrected mesh:

- The shapes of the corrected cells are close to the exact Lagrangian shapes
- The barycenters of the corrected cells are close to the exact barycenters

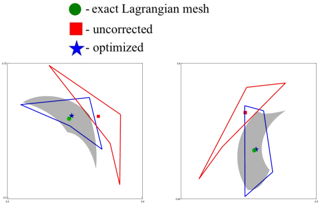

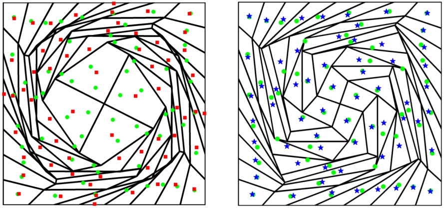

Improvements in Mesh Geometry

We observe significant improvements in the geometry of the corrected mesh:

- The shapes of the corrected cells are close to the exact Lagrangian shapes
- The barycenters of the corrected cells are close to the exact barycenters
- The trajectories of the corrected cells are close to the exact Lagrangian trajectories

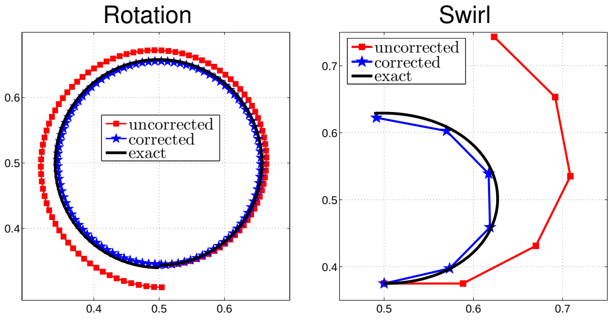

Application to Semi-Lagrangian Transport

Given cell volume $c_i = \int_{\kappa_i} dV$, cell mass $m_i = \int_{\kappa_i} \rho(\mathbf{x}, t) dV$, and cell average density $\rho_i = m_i / c_i$ at time t

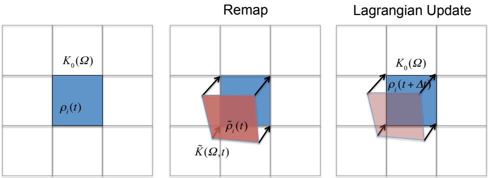

1. Define Lagrangian departure cells: $c_i \to \tilde{c}_i$
2. Remap from fixed grid to departure grid: $\rho_i \to \tilde{\rho}_i$, $\tilde{m}_i = \tilde{\rho}_i \tilde{c}_i$
3. Lagrangian update: $m_i(t + \Delta t) = \tilde{m}_i$, $\rho_i(t + \Delta t) = m_i(t + \Delta t)/c_i$

Application to Semi-Lagrangian Transport

Given cell volume $c_i = \int_{\kappa_i} dV$, cell mass $m_i = \int_{\kappa_i} \rho(\mathbf{x}, t) dV$, and cell average density $\rho_i = m_i / c_i$ at time t

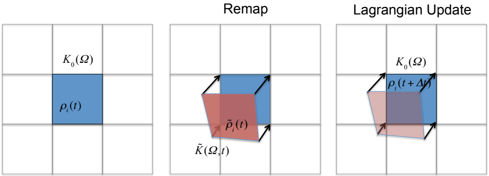

1. Define Lagrangian departure cells: $c_i \rightarrow \hat{c}_i$
2. Volume correction: $\hat{c}_i \rightarrow \tilde{c}_i$
3. Remap from fixed grid to departure grid: $\rho_i \rightarrow \tilde{\rho}_i,\ \tilde{m}_i = \tilde{\rho}_i \tilde{c}_i$
4. Lagrangian update: $m_i(t + \Delta t) = \tilde{m}_i,\ \rho_i(t + \Delta t) = m_i(t + \Delta t)/c_i$

Application to Semi-Lagrangian Transport

Given cell volume $c_i = \int_{\kappa_i} dV$, cell mass $m_i = \int_{\kappa_i} \rho(\mathbf{x}, t) dV$, and cell average density $\rho_i = m_i / c_i$ at time t

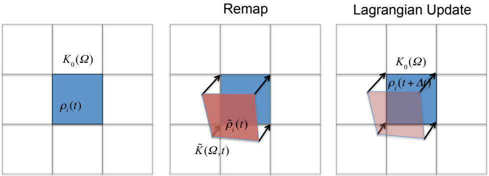

1. Define Lagrangian departure cells: $c_i \to \hat{c}_i$
2. Volume correction: $\hat{c}_i \to \tilde{c}_i$
3. Remap from fixed grid to departure grid: $\rho_i \to \tilde{\rho}_i, \ \tilde{m}_i = \tilde{\rho}_i \tilde{c}_i$
4. Lagrangian update: $m_i(t + \Delta t) = \tilde{m}_i, \ \rho_i(t + \Delta t) = m_i(t + \Delta t)/c_i$

We use linear reconstruction of density with Van Leer limiting for remap.

Dukowicz and Baumgardner, Incremental remapping as a transport/advection algorithm, *JCP* 2000.

Semi-Lagrangian Transport Results

Constant density, rotational flow

Uncorrected

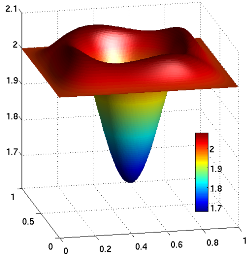

Corrected

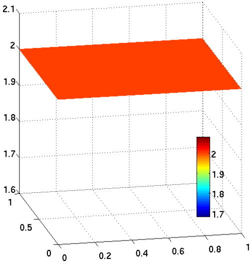

Comparison

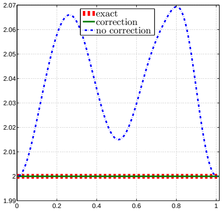

Forward Euler with $\Delta t = 0.006$.

Semi-Lagrangian Transport Results

Cylindrical density, rotational flow

Uncorrected

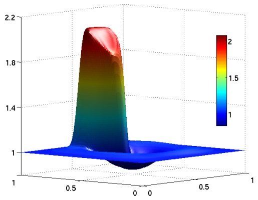

Corrected

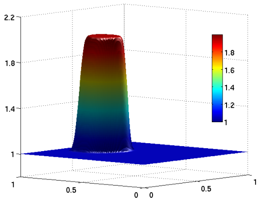

Comparison

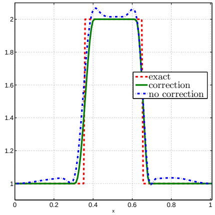

Forward Euler with $\Delta t = 0.006$.

Multi-Material Semi-Lagrangian Transport

Consider transport of volume fraction of material s

$$\frac{\partial T_s}{\partial t} + \nabla \cdot (T_s \boldsymbol{u}) = 0, \quad s = 1, \ldots, S,$$

$$T_{s,i}(t) = \frac{\int_{\kappa_i(t)} T_s \, dV}{\int_{\kappa_i(t)} dV} = \frac{|\kappa_{s,i}(t)|}{|\kappa_i(t)|}$$

3 material, swirling velocity

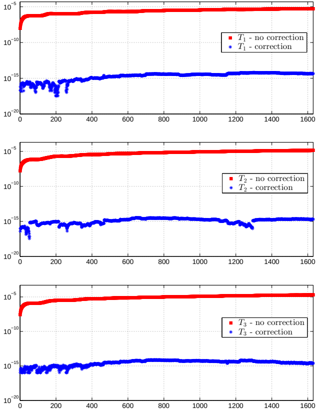

$$|\Omega_s^n| = \sum_{i=1}^{m} T_{s,i}^n |\kappa_i|$$

Conclusions

Presented a new approach for improving the accuracy and physical fidelity of numerical schemes that rely on Lagrangian mesh motion

- Optimization-based volume correction
  - Is computationally efficient
  - Provides significant geometric improvments in corrected meshes
  - Enables semi-Lagrangian transport methods to preserve volumes and constant densities
- Future work
  - Further development of mesh quality constraints and rigorous enforcement of mesh validity
  - Investigate utility of algorithm for mesh quality improvement